

# Enzastaurin (LY317615), a protein kinase C $\beta$ inhibitor, inhibits the AKT pathway and induces apoptosis in multiple myeloma cell lines

Mujahid A. Rizvi,<sup>1,2</sup> Kulsoom Ghias,<sup>2</sup>  
Katharine M. Davies,<sup>2</sup> Chunguang Ma,<sup>2</sup>  
Frank Weinberg,<sup>2</sup> Hidayatullah G. Munshi,<sup>1,2</sup>  
Nancy L. Krett,<sup>2</sup> and Steven T. Rosen<sup>1,2</sup>

<sup>1</sup>Division of Hematology/Oncology, Department of Medicine, Northwestern University Feinberg School of Medicine and <sup>2</sup>Robert H. Lurie Comprehensive Cancer Center of Northwestern University, Chicago, Illinois

## Abstract

Enzastaurin (LY317615), an acyclic bisindolylmaleimide, is an oral inhibitor of the protein kinase C $\beta$  isozyme. The objective of this study was to assess the efficacy of enzastaurin in inducing apoptosis in multiple myeloma (MM) cell lines and to investigate possible mechanisms of apoptosis. Cell proliferation assays were done on a variety of MM cell lines with unique characteristics (dexamethasone sensitive, dexamethasone resistant, chemotherapy sensitive, and melphalan resistant). The dexamethasone-sensitive MM.1S cell line was used to further assess the effect of enzastaurin in the presence of dexamethasone, insulin-like growth factor-I (IGF-I), interleukin-6, and the pan-specific caspase inhibitor ZVAD-fmk. Enzastaurin increased cell death in all cell lines at clinically significant low micromolar concentrations (1–3  $\mu$ mol/L) after 72 hours of treatment. Dexamethasone and enzastaurin were shown to have an additive effect on MM.1S cell death. Although IGF-I blocked the effect of 1  $\mu$ mol/L enzastaurin, IGF-I did not abrogate cell death induced with 3  $\mu$ mol/L enzastaurin. Moreover, enzastaurin-induced cell death was not affected by interleukin-6 or ZVAD-fmk. GSK3 $\beta$  phosphorylation, a reliable pharmacodynamic marker for enzastaurin activity, and AKT phosphorylation were both decreased with enzastaurin treatment. These data indicate that enzastaurin induces apoptosis in MM cell lines in a caspase-independent manner and that enzastaurin exerts its antimyeloma effect by inhibiting signaling through the AKT pathway. [Mol Cancer Ther 2006;5(7):1783–9]

Received 11/8/05; revised 4/9/06; accepted 5/10/06.

The costs of publication of this article were defrayed in part by the payment of page charges. This article must therefore be hereby marked advertisement in accordance with 18 U.S.C. Section 1734 solely to indicate this fact.

**Requests for reprints:** Mujahid A. Rizvi, Division of Hematology/Oncology, Department of Medicine, Northwestern University Feinberg School of Medicine, Lurie Building 3-250, 303 East Superior Street, Chicago, IL 60611. Phone: 312-695-6180; Fax: 312-695-6189. E-mail: m-rizvi@md.northwestern.edu

Copyright © 2006 American Association for Cancer Research.

doi:10.1158/1535-7163.MCT-05-0465

## Introduction

Multiple myeloma (MM) is characterized by malignant transformation and proliferation of a single clone of plasma cells that produce a monoclonal immunoglobulin. MM accounts for 10% of all hematologic malignancies and 1% of all malignant disease in the United States (1). The annual incidence of MM is 4 per 100,000 (1). In the last decade, the treatment of MM has evolved rapidly. The use of high-dose chemotherapy followed by autologous stem cell transplant has increased remission rates and progression-free survival, and overall survival compared with conventional chemotherapy (2). Unfortunately, a large proportion of patients relapse, and the search for new, more effective salvage therapies is needed.

The protein kinase C (PKC) family consists of 11 serine/threonine protein kinase isoforms that are involved in cell proliferation and differentiation, gene transcription, and tumor-induced angiogenesis. The PKC pathway has been shown to play a role in the regulation of cell growth in hematologic malignancies. In diffuse large B-cell lymphoma, oligonucleotide microarray gene expression profiles were used to predict outcomes and PKC $\beta$  was found to be overexpressed in refractory/fatal cases of diffuse large B-cell lymphoma (3, 4). In MM, the role of the PKC pathway has not been extensively studied; however, there is some evidence that MM cell migration may in fact be modulated by the vascular endothelial growth factor via a PKC-dependent pathway (5). Ni and colleagues (6) showed that the U266, RPMI8226S, and K620 MM cell lines expressed PKC $\delta$ , PKC $\iota$ , PKC $\mu$ , and PKC $\zeta$ . PKC $\beta$  was expressed in the RPMI8226S and K620 cell lines, but not in the U266 cell line. In addition, the K620 cell line expressed PKC $\alpha$ , PKC $\gamma$ , PKC $\epsilon$ , and PKC $\theta$ . The U266 cell line was treated with safingol, a general PKC inhibitor, and rottlerin, a PKC $\delta$  specific inhibitor, and both induced apoptosis in MM cells (6). A phase II trial using bryostatin 1, a PKC modulator, was conducted in MM patients; although the treatment was well tolerated, none of the nine patients responded (7).

Enzastaurin (LY317615), an acyclic bisindolylmaleimide, is an oral inhibitor of the PKC $\beta$  isozyme. In a phase I clinical trial, patients treated with 525 mg/d enzastaurin achieved steady-state plasma concentrations of 8  $\mu$ mol/L, with a mean plasma exposure of 2  $\mu$ mol/L (8). Enzastaurin selectively inhibits PKC $\beta$  at low concentrations, but also inhibits the other PKC isozymes at concentrations achieved physiologically in clinical trials. It does not inhibit other cellular serine/threonine kinases and tyrosine kinases, such as, I $\kappa$ B kinase  $\alpha$ , I $\kappa$ B kinase  $\beta$ , c-Jun-NH<sub>2</sub>-kinase, mitogen-activated protein kinase kinase, stress-activated protein kinase, mitogen-activated protein kinase, AMP-activated

protein kinase, PRK2, PKB $\alpha$ , PKB $\beta$ , PDK1, epidermal growth factor receptor, platelet-derived growth factor receptor, fibroblast growth factor receptor, Bruton's tyrosine kinase, SRC, and Abl (9). PKC $\beta$  is a part of the signal cascade of vascular endothelial growth factor; therefore, initial data has focused on the effects of enzastaurin on angiogenesis. Because there is data to suggest that gliomas are dependent on vascular endothelial growth factor-mediated angiogenesis, a phase II trial of enzastaurin in high-grade gliomas is currently under way. Eighty-five patients have been treated with enzastaurin and 79 patients are evaluable for response. Seventy-two percent of the patients had glioblastoma multiforme. Treatment with enzastaurin was well tolerated with minimal drug-related toxicity: three patients had grade 3 to 4 hematologic toxicity and one patient had grade 2 hepatotoxicity. Thirty-six patients received more than one cycle of enzastaurin and 13 of these patients had stable disease for >3 months. Objective radiographic responses have been seen in 14 patients (10 glioblastoma multiforme patients), one of whom had a complete response and is still receiving enzastaurin 13 months after enrollment (10).

In addition to the anti-vascular endothelial growth factor effects, enzastaurin in the low- $\mu$ mol/L range has been shown to suppress proliferation in a wide variety of cancer cell lines: leukemia, non-small cell lung cancer, colon cancer, melanoma, ovarian cancer, renal cancer, prostate cancer, and breast cancer cell lines (9). Graff et al. (9) have shown that enzastaurin (1–4  $\mu$ mol/L) induces apoptosis in the HCT116 colon carcinoma cell line and U87MG glioblastoma cells. In addition, they have shown a time-dependent loss of GSK3 $\beta$  phosphorylation after exposure to enzastaurin (1–3  $\mu$ mol/L) in the colon cancer cell line, U87MG glioblastoma cells, and in xenograft-bearing mice. A similar loss of GSK3 $\beta$  phosphorylation was seen in the mouse peripheral blood mononuclear cells and xenograft tissues. GSK3 $\beta$  phosphorylation is associated with PKC $\beta$  activity directly and is also a downstream target of the AKT pathway. They concluded that enzastaurin may exert its antineoplastic effects by inhibiting the AKT pathway and further that GSK3 $\beta$  phosphorylation is a reliable pharmacodynamic marker for enzastaurin activity. We were able to corroborate these findings with enzastaurin in cutaneous T-cell lymphoma cell lines (HuT-78 and CRL-2105; ref. 11).

Here, we show that enzastaurin induces apoptosis in MM cell lines at concentrations achieved in phase I clinical trials. We also show the loss of GSK3 $\beta$  and AKT phosphorylation when myeloma cells are exposed to enzastaurin.

## Materials and Methods

### Chemicals

Enzastaurin was obtained from Eli Lilly and Co. (Indianapolis, IN). Interleukin-6 (IL-6), insulin-like growth factor-I (IGF-I), and ZVAD-fmk was purchased from R&D Systems (Minneapolis, MN). Dexamethasone was obtained from Sigma (St. Louis, MO).

### Cell Culture

A variety of MM cell lines with unique characteristics were used. MM.1S is a glucocorticoid-sensitive cell line established from the peripheral blood of a MM patient (12). MM.1R<sub>e</sub> (1.414) and MM.1R<sub>L</sub> are subclones of MM.1S with partial to complete resistance to glucocorticoids. The U266 cell line is also resistant to glucocorticoids. RPMI8226S is a chemotherapy-sensitive cell line, whereas RPMI8226-LR 5 (selected with melphalan) is a chemotherapy-resistant cell line. The chemotherapy-sensitive and chemotherapy-resistant cell lines were provided by Dr. William Dalton (H. Lee Moffitt Cancer Center and Research Institute, Tampa, FL).

MM cell lines were cultured in RPMI 1640 (Life Technologies, Inc., Grand Island, NY) supplemented with 10% fetal bovine serum (HyClone, Inc., Logan, UT), 2 mmol/L glutamine, 100 units/mL penicillin, 100  $\mu$ g/mL streptomycin, 5  $\mu$ g/mL plasmocin, and 2.5  $\mu$ g/mL fungizone. Cells were maintained at 37°C in an incubator with 5% CO<sub>2</sub>. These cell lines have a doubling time of ~72 hours.

### Enzastaurin Treatment

Twenty-four hours before treatment with enzastaurin, the myeloma cell lines were transferred to RPMI 1640 with 1% fetal bovine serum due to the high protein binding affinity of enzastaurin (concentration of glutamine, penicillin, streptomycin, plasmocin, and fungizone were kept constant; ref. 9). The MM cells were seeded into culture at concentrations that would ensure logarithmic growth over the duration of the experiment. The concentration and time of treatment with enzastaurin is detailed in the individual experiments. The cells were maintained in standard culture conditions over the course of the experiment. To determine whether enzastaurin-induced apoptosis was caspase-dependent, ZVAD-fmk, a pan-specific caspase inhibitor, was used at 40  $\mu$ mol/L. ZVAD-fmk was always added 1 hour before enzastaurin treatment.

### Cell Proliferation Assay

MM cells were cultured into 96-well dishes at a concentration of 25,000 per well and incubated with the indicated drugs for 72 hours. Cell proliferation was determined using the 3-(4,5-dimethylthiazol-2-yl)-5-(3-carboxymethoxyphenyl)-2-(4-sulfophenyl)-2H-tetrazolium Cell Titer Aqueous assay (Promega, Madison, WI), which measured the conversion of a tetrazolium compound into formazan by a mitochondrial dehydrogenase enzyme in live cells. The amount of formazan is proportional to the number of living cells present in the assay mixture. Each data point was the average of four independent determinations. The data were expressed as the percentage of formazan produced by the untreated cells in the same assay.

### Immunoblotting Analysis

MM cells were cultured and grown at a concentration of  $1 \times 10^6$ /mL. Cells were treated and harvested at the desired time points. Cell pellets were homogenized in lysis buffer [10 mmol/L KPO<sub>4</sub> (pH 7.0), 1 mmol/L EDTA, 5 mmol/L EGTA, 10 mmol/L MgCl<sub>2</sub>, 50 mmol/L B-glycerol phosphate, 1 mmol/L sodium orthovanadate, 2 mmol/L DTT, 1 mmol/L phenylmethylsulfonyl fluoride, 0.5% NP40, and 0.1% deoxycholate]. Homogenates were centrifuged at 4°C

for 10 minutes at  $16,100 \times g$ , the supernatants were collected, and protein concentrations were determined by Bio-Rad protein assay (Bio-Rad Laboratories, Hercules, CA). Thirty micrograms of protein were loaded with sample buffer [125 mmol/L Tris (pH 6.8), 4% SDS, 20% glycerol, 100 mmol/L DTT, and 0.05% bromphenol blue] onto a precast 8% to 16% Tris-glycine gels (Invitrogen/Novex, Carlsbad, CA). Proteins were then transferred to a polyvinylidene difluoride membrane (Immobilon-P; Millipore, Bedford, MA). After protein transfer, membranes were blocked with 5% bovine serum albumin in TBS for at least 1 hour and subsequently incubated with the appropriate primary antibody at a 1:1,000 dilution overnight at 4°C. Phospho-GSK3 $\beta$ <sup>(serine9)</sup>, GSK3 $\beta$ , and AKT antibody were purchased from Cell Signaling Technologies (Beverly, MA). To detect poly(ADP-ribose)polymerase (PARP), a mouse monoclonal antibody was used (BD PharMingen, San Diego, CA). Phospho-AKT<sup>(serine473)</sup> antibody was purchased from R&D Systems (Minneapolis, MN). The R&D Systems antibody required a different blocking solution that contained 5% nonfat dry milk, 25 mmol/L Tris, 0.15 mol/L NaCl, and 0.1% Tween 20 (pH 7.4). A primary antibody concentration of 0.5  $\mu\text{g}/\text{mL}$  was used for the phospho-AKT<sup>(serine473)</sup> antibody. The following day, blots were washed with TBS-T (TBS with 0.1% Tween 20) and incubated for 1 hour at room temperature with a 1:5,000 dilution of horseradish peroxidase-linked secondary antibody (Amersham, Arlington Heights, IL). After washing the blots with TBS-T, they were developed using enhanced chemiluminescence (ECL Plus; Amersham), and the signal was visualized with X-ray film (Hyperfilm; Amersham).

#### Cell Cycle Analysis

Cells ( $2 \times 10^6$ ) were treated with enzastaurin at the concentration indicated in the figure legends. After incubation for 72 hours, cells were collected, centrifuged at  $500 \times g$ , washed with cold PBS, and fixed overnight with 40% ethanol at 4°C. Cells were washed with cold PBS, and the pellet was resuspended in 50  $\mu\text{g}/\text{mL}$  RNase A (diluted in PBS), and incubated for 30 minutes at 37°C. The samples were then resuspended in 25  $\mu\text{g}/\text{mL}$  propidium iodide in 38 mmol/L sodium citrate buffer. Flow cytometry was done on a Coulter EPICs XL instrument and data were analyzed using the System II software package.

#### Annexin V Staining

Cells ( $1 \times 10^6/\text{mL}$ ) were treated with 3  $\mu\text{mol}/\text{L}$  enzastaurin and harvested after 72 hours. As cells undergo apoptosis, the integrity of the cell membrane is disrupted and phosphatidylserine is exposed. Detection of phosphatidylserine on the outer leaflet of apoptotic cells was done by using Annexin V binding according to the instructions of the manufacturer (BD PharMingen). Briefly, cells were incubated with 5  $\mu\text{g}/\text{mL}$  FITC-conjugated Annexin V in the presence of 5  $\mu\text{g}/\text{mL}$  propidium iodide and screened by flow cytometry (Coulter EPICs XL). Annexin V-FITC positive, PI-negative cells were scored as early apoptotic. Annexin V-FITC positive, PI-positive cells were scored as late apoptotic.

#### Statistical Analysis

Data were analyzed using GraphPad InStat statistical software (GraphPad Software, Inc., San Diego, CA). Unpaired *t* tests were done and two-tailed *P* values are reported.

## Results

### Enzastaurin Inhibits Cell Proliferation in MM Cell Lines

MM.1S, MM.1R<sub>e</sub>, MM.1R<sub>L</sub>, RPMI8226S, RPMI8226-LR5, and U266 MM cell lines were treated with increasing concentrations of enzastaurin. The cell proliferation assay, as described in Materials and Methods, was measured after 24 and 72 hours of treatment with enzastaurin. There was no evidence of inhibition of cell growth at clinically relevant concentrations at 24 hours (data not shown). At 72 hours, there was evidence of decreased cell proliferation at low  $\mu\text{mol}/\text{L}$  concentrations (1–3  $\mu\text{mol}/\text{L}$ ; Fig. 1). The mean percentage of viable cells present after 72 hours of treatment with 3  $\mu\text{mol}/\text{L}$  enzastaurin was 40% (range 18–81%). The RPMI8226S (chemotherapy sensitive) and the RPMI8226-LR5 (chemotherapy resistant) cell lines were more resistant to enzastaurin, with 61% and 81% viable cells present, respectively, after 72 hours of exposure to 3  $\mu\text{mol}/\text{L}$  enzastaurin.

### Enzastaurin and Dexamethasone Show Additive, Not Synergistic, Effects

MM.1S cells were treated with increasing concentrations of enzastaurin. Using cell cycle analysis, we determined the fraction of cells in the sub-G<sub>1</sub> phase, indicating cells undergoing apoptosis (Fig. 2A). The percentage of cells undergoing apoptosis increased with increasing concentrations of enzastaurin. After 72 hours of exposure to 3  $\mu\text{mol}/\text{L}$  enzastaurin, there was a 2.7-fold (52% of cells in the sub-G<sub>1</sub> phase) increase in the proportion of cells in the sub-G<sub>1</sub> phase compared with untreated controls (18.7% of

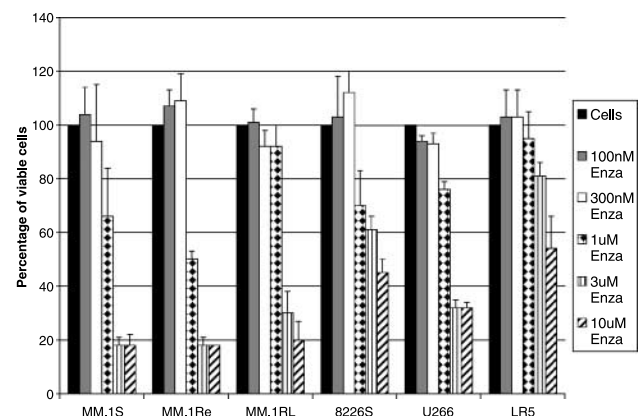


**Figure 1.** Enzastaurin treatment decreases the number of viable cells. MM cell lines were treated with increasing concentrations of enzastaurin (Enza) for 72 h. The cell proliferation assay measured the amount of formazan, which is directly proportional to the number of living cells present compared with the control.

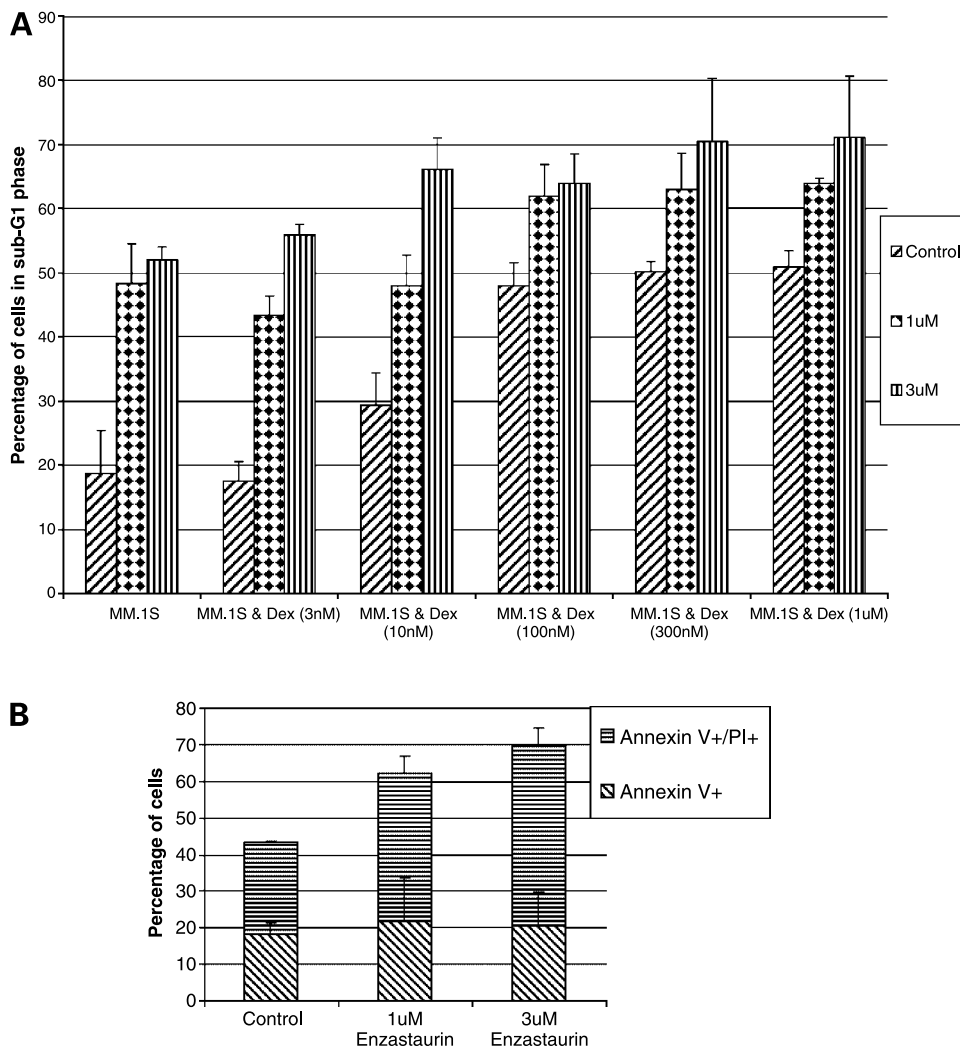


**Figure 2.** Enzastaurin treatment induces apoptosis in MM cells. **A**, MM.1S cells were treated with increasing concentrations of enzastaurin for 72 h. The same set of experiments was repeated with increasing concentrations of dexamethasone (*Dex*) simultaneously with enzastaurin. DNA content was measured by staining with propidium iodide followed by flow cytometry as described in Materials and Methods. **B**, MM.1S cells were treated with increasing concentrations of enzastaurin for 72 h. Annexin V staining was determined by flow cytometry as described in Materials and Methods. *PI*, propidium iodide.

cells in the sub- $G_1$  phase). The same set of experiments was repeated with the addition of increasing concentrations of dexamethasone simultaneously with enzastaurin (Fig. 2A). There was no evidence that low doses of dexamethasone (3 nmol/L) had any effect on MM.1S cells (percentage of cells in the sub- $G_1$  phase was 17.6% compared with 18.7% in the control). We were unable to show synergistic effects between suboptimal doses of dexamethasone and clinically relevant doses (1–3  $\mu$ mol/L) of enzastaurin (percentage of cells in the sub- $G_1$  phase was 55.9% with 3 nmol/L dexamethasone and 3  $\mu$ mol/L enzastaurin and 52% with 3  $\mu$ mol/L enzastaurin). There was, however, evidence of an additive effect at higher concentrations of dexamethasone and enzastaurin (1–3  $\mu$ mol/L).

We used a parallel assay to determine whether cell cycle analysis was accurate in determining the percentage of cells undergoing apoptosis. We used Annexin V–FITC binding as a confirmatory assay. The cell cycle analysis was a more conservative assay in determining the percentage of cells undergoing apoptosis (Fig. 2B).

#### IGF-I Partially Inhibits the Effects of Enzastaurin on MM.1S Cells whereas IL-6 Has No Effect

IL-6 has pleiotropic effects on hematopoietic and non-hematopoietic cells and is an important growth factor for MM cells (13, 14). IL-6 facilitates B-cell differentiation into immunoglobulin-secreting plasma cells and has been shown to prevent drug-induced apoptosis (15). IGF-I is a crucial growth and survival factor for MM (16) and has been shown to inhibit dexamethasone-induced apoptosis (17). Cell cycle analysis was used to determine whether either IL-6 or IGF-I could affect enzastaurin-induced apoptosis. Cells were treated with 1 and 3  $\mu$ mol/L enzastaurin for 72 hours with or without IL-6 (1 ng/mL). In a similar fashion, MM.1S cells were treated with enzastaurin in the presence or absence of IGF-I (100 ng/mL). Enzastaurin-induced apoptosis was not affected by the addition of IL-6 (Fig. 3A and B). There was a 3.4-fold increase in the percentage of cells in the sub- $G_1$  phase with 3  $\mu$ mol/L enzastaurin irrespective of whether IL-6 was present or not. Experiments were done using higher concentrations of IL-6 (5 and 50 ng/mL) with similar

results (data not shown). In contrast, IGF-I inhibits enzastaurin-induced apoptosis at lower concentrations of enzastaurin (1  $\mu\text{mol/L}$ ). Forty-eight percent of cells were in the sub- $G_1$  phase after a 72-hour exposure to 1  $\mu\text{mol/L}$  enzastaurin compared with 22% of cells with 1  $\mu\text{mol/L}$  enzastaurin and 100 ng/mL IGF-I ( $P = 0.048$ ). However, a higher concentration of enzastaurin (3  $\mu\text{mol/L}$ ) was able to overcome the inhibitory effects of IGF-I ( $P = 0.24$ ; Fig. 3A and B).

#### Enzastaurin Induces Apoptosis in a Caspase-Independent Manner

PARP is a 116 kDa protein that is a substrate for activated caspase-3. The cleaved form of PARP is detected

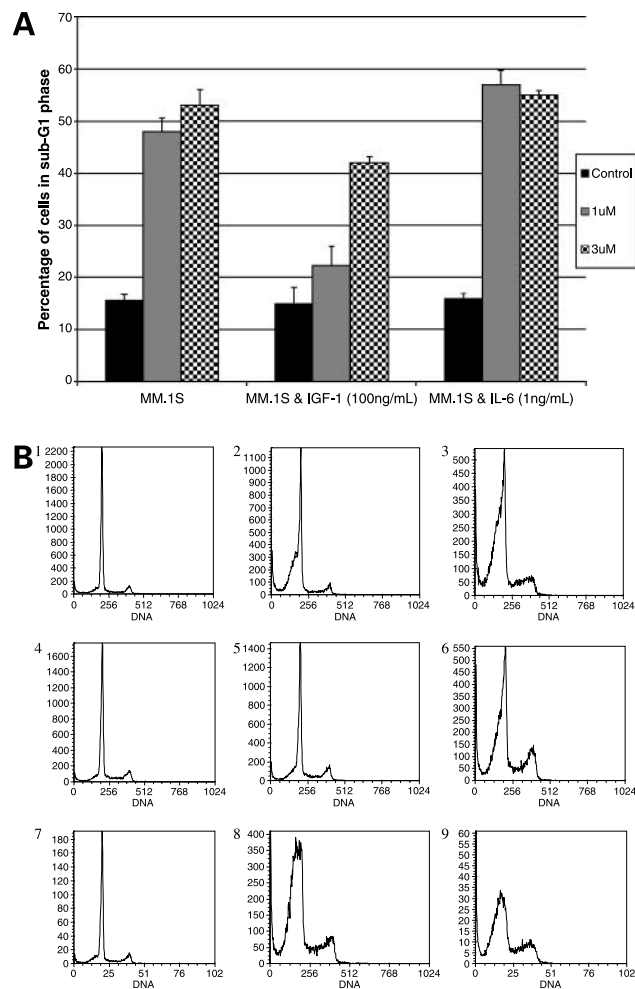


**Figure 3.** Effect of MM growth factors on enzastaurin-induced apoptosis. **A**, enzastaurin treatment induces apoptosis in MM cells by virtue of increased sub- $G_1$  phase cell population. MM.1S cells were treated with increasing concentrations of enzastaurin for 72 h. The same set of experiments was repeated separately with the addition of IL-6 (1 ng/mL) and IGF-I (100 ng/mL). DNA content was measured by staining with propidium iodide followed by flow cytometry as described in Materials and Methods. **B**, representative flow cytograms. 1, control; 2, 1  $\mu\text{mol/L}$  enzastaurin; 3, 3  $\mu\text{mol/L}$  enzastaurin; 4, 100 ng/mL IGF-I; 5, 100 ng/mL IGF-I and 1  $\mu\text{mol/L}$  enzastaurin; 6, 100 ng/mL IGF-I and 3  $\mu\text{mol/L}$  enzastaurin; 7, 1 ng/mL IL-6; 8, 1 ng/mL IL-6 and 1  $\mu\text{mol/L}$  enzastaurin; 9, 1 ng/mL IL-6 and 3  $\mu\text{mol/L}$  enzastaurin.

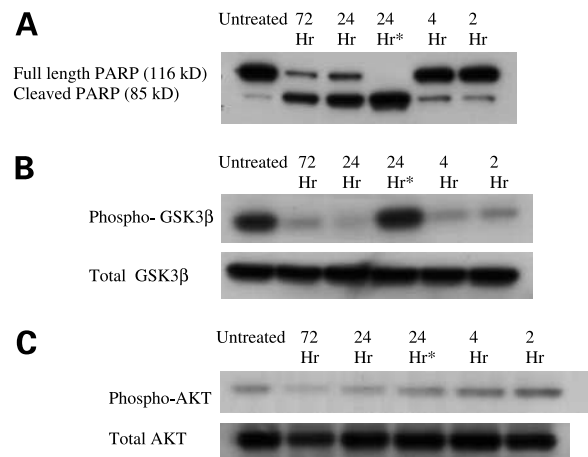


**Figure 4.** Effect of enzastaurin on PARP cleavage and kinase phosphorylation. MM.1S cells were treated with enzastaurin (2  $\mu\text{mol/L}$ ) for the indicated times. **A**, cleavage of PARP in enzastaurin-treated cells. \*, 1  $\mu\text{mol/L}$  dexamethasone. **B**, decrease in phosphorylation of GSK3 $\beta$ . \*, 1  $\mu\text{mol/L}$  dexamethasone. **C**, decrease in phosphorylation of AKT. \*, 1  $\mu\text{mol/L}$  dexamethasone. Whole cell lysates were prepared and immunoblotted for PARP, phospho-GSK3 $\beta$  and total GSK3 $\beta$ , and phospho and total AKT as described in Materials and Methods. Immunoblots are representative of two similar experiments.

at 85 kDa by immunoblotting. Cells were treated with enzastaurin (2  $\mu\text{mol/L}$ ) for the indicated times, harvested, and whole cell extracts were prepared, fractionated, and immunoblotted as described. As shown in Fig. 4A, immunoblots of whole cell lysates of MM.1S cells treated with enzastaurin for 2, 4, 24, and 72 hours showed PARP cleavage as early as 24 hours of incubation. Dexamethasone was used as a positive control because it is known to induce apoptosis in MM.1S cells, and there was evidence of PARP cleavage after a 24-hour exposure to dexamethasone (1  $\mu\text{mol/L}$ ).

Cell cycle analysis was used to further elucidate the role of caspase activation in enzastaurin-induced apoptosis in MM cells. MM.1S cells were treated with enzastaurin (1 and 3  $\mu\text{mol/L}$ ) for 72 hours as described in the above experiments in the presence and absence of ZVAD-fmk (40  $\mu\text{mol/L}$ ), a pan-specific caspase inhibitor added 1 hour before enzastaurin. The percentage of cells in the sub- $G_1$  phase in the untreated control and the ZVAD-fmk-treated control was 27% and 18%, respectively (Fig. 5). This indicated that there was caspase-dependent apoptosis present in MM.1S cells at baseline. After treatment with enzastaurin (3  $\mu\text{mol/L}$  for 72 hours), the percentage of cells undergoing apoptosis in the ZVAD-fmk-untreated (57%) and ZVAD-fmk-treated cells (51%) was similar ( $P = 0.28$ ). Dexamethasone-induced apoptosis is caspase dependent. We treated MM.1S cells with 1  $\mu\text{mol/L}$  dexamethasone in the presence and absence of ZVAD-fmk (40  $\mu\text{mol/L}$ ). There was a 40% decrease in the relative number of cells undergoing apoptosis in the ZVAD-fmk-treated samples ( $P < 0.01$ ). Our data suggest that enzastaurin-induced apoptosis may be caspase independent.

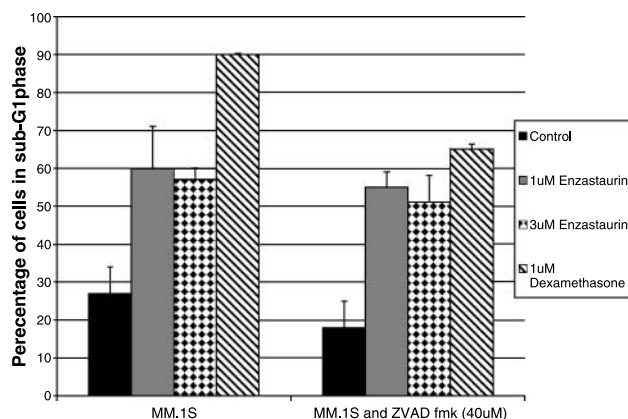


**Figure 5.** Enzastaurin induces caspase-independent apoptosis. Enzastaurin treatment induces apoptosis in MM cells by virtue of increased sub-G<sub>1</sub>-phase cell population. MM.1S cells were treated with increasing concentrations of enzastaurin. ZVAD-fmk was added 1 h before the addition of enzastaurin. DNA content was measured by staining with propidium iodide followed by flow cytometry as described in Materials and Methods.

### Enzastaurin Decreases Phosphorylation of GSK3 $\beta$ and AKT

GSK3 $\beta$  is a pharmacodynamic marker for enzastaurin and has been linked to PKC $\beta$  directly and is also a downstream target of the AKT pathway. MM.1S cells were treated with 2  $\mu$ mol/L enzastaurin for 2, 4, 24, and 72 hours. The cells were harvested, and whole cell extracts were prepared, fractionated, and immunoblotted as described in Materials and Methods. Dexamethasone was used as a negative control and there was no evidence of loss of phosphorylation of GSK3 $\beta$ <sup>(serine9)</sup> or AKT<sup>(serine473)</sup> after a 24-hour exposure to dexamethasone (1  $\mu$ mol/L). Enzastaurin treatment showed a distinct, time-dependent reduction of GSK3 $\beta$ <sup>(serine9)</sup> and AKT<sup>(serine473)</sup> phosphorylation, whereas total protein levels remain unchanged (Fig. 4B and C). We conclude that enzastaurin may exert its antimyeloma activity by inhibiting the PKC $\beta$  and AKT pathway.

### Discussion

There are ~13,700 new patients diagnosed with MM and almost 11,000 patients succumb to this illness every year in the United States (1). It is only recently that progress has been made in terms of survival in patients with MM. Unfortunately, the course of the disease is characterized by frequent relapses and development of resistance to chemotherapy and other agents. Therefore, it is imperative that newer agents with novel mechanisms of action be tested in MM. Here, we have evaluated the effects of enzastaurin in MM cell lines and investigated possible mechanisms by which it exerts its effects.

PKC act by regulating cell growth and differentiation in hematopoietic cells by modulating signal transduction (18–20). The data on PKC effects in MM cells, however,

is limited. Recent reports in the literature describe a role for PKC in AKT activity. PKC $\beta$ II can phosphorylate AKT at serine 473 and activate AKT (21). Graff et al. (9) present evidence that enzastaurin may affect human tumor cells, directly inducing a loss of phosphorylation of GSK3 $\beta$ , and AKT in a colon cancer cell line (HCT 116). We have shown a time-dependent loss of phosphorylation of GSK3 $\beta$  and AKT in the MM.1S cell line. A decrease in AKT phosphorylation was seen at 24 hours, a time at which cleavage of the PARP protein is detected. This also correlates with our findings and those of Graff et al. (9) who found evidence of significant apoptosis with enzastaurin after 72 hours of exposure. The loss of GSK3 $\beta$  at an earlier time point may have been due to PKC inhibition alone.

Enzastaurin is an oral agent given once daily. In phase I clinical trials, it was well tolerated with minimal adverse events (8). The efficacy of enzastaurin in MM cell lines, the MM.1S cell line in particular, makes it an attractive agent for further evaluation. We have shown enzastaurin-induced apoptosis in MM cells at clinically significant concentrations (1–3  $\mu$ mol/L). We have also shown an additive effect with enzastaurin and dexamethasone, a commonly used drug in MM. Our investigation revealed that the effects of enzastaurin are not suppressed in the presence of IL-6 *in vitro*. This held true in the face of higher concentrations of IL-6. IGF-I, however, inhibits enzastaurin-induced apoptosis at lower concentrations (1  $\mu$ mol/L). The inhibitory effects of IGF-I were reversed at higher concentrations of enzastaurin (3  $\mu$ mol/L). Mitsiades et al. (22) have previously shown that IGF-I promotes MM cell growth by stimulating the activation of NF- $\kappa$ B and AKT in MM cell lines. In contrast, IL-6 does not activate NF- $\kappa$ B and induces less AKT activity compared with IGF-I (22). Our data is consistent with their findings because only IGF-I was able to inhibit enzastaurin-induced apoptosis. This has therapeutic implications and may prove beneficial in patients who have relapsed or refractory disease by targeting MM cells through different mechanisms.

The results of this study provide a platform for further evaluation of the role of PKCs in the pathogenesis of MM and the role of enzastaurin in the treatment of MM. It would be interesting to evaluate microarray gene expression profiles and chromosomal analyses of patients with MM to see whether the expression of PKC $\beta$  was associated with poor prognostic factors and sensitivity to antimyeloma agents. We are currently in the process of initiating a phase II trial with enzastaurin in MM patients. In addition to studying the effects of enzastaurin in patients, further studies to elucidate the role of PKCs in the pathogenesis of MM will be done.

### Acknowledgments

We thank Mary Paniagua and Jeff Nelson.

### References

- Landis SH, Murray T, Bolden S, Wingo PA. Cancer statistics. CA Cancer J Clin 1999;49:8–31.

2. Attal M, Harousseau JL, Stoppa AM, et al. A prospective, randomized trial of autologous bone marrow transplantation and chemotherapy in multiple myeloma. Intergroupe Francais du Myelome. *N Engl J Med* 1996; 335:91–7.
3. Shipp MA, Ross KN, Tamayo P, et al. Diffuse large B-cell lymphoma outcome prediction by gene-expression profiling and supervised machine learning. *Nat Med* 2002;8:68–74.
4. Wu E, Aguiar RC, Savage K, et al. A rational therapeutic target in diffuse large B-cell lymphoma. *Blood* 2002;100:757a.
5. Podar K, Tai YT, Davies FE, et al. Vascular endothelial growth factor triggers signaling cascades mediating multiple myeloma cell growth and migration. *Blood* 2001;98:428–35.
6. Ni H, Ergin M, Tibudan SS, Denning MF, Izban KF, Alkan S. Protein kinase C- $\delta$  is commonly expressed in multiple myeloma cells and its downregulation by rottlerin causes apoptosis. *Br J Haematol* 2003;121: 849–56.
7. Varterasian ML, Pemberton PA, Hulburd K, Rodriguez DH, Murgo A, Al-Katib AM. Phase II study of bryostatins 1 in patients with relapsed multiple myeloma. *Invest New Drugs* 2001;19:245–7.
8. Herbst R, Thornton DE, Kies MS, et al. Phase I study of LY317615, a protein kinase C $\beta$  inhibitor. *Proc Am Soc Clin Oncol* 2002;20:82a.
9. Graff JR, McNulty AM, Hanna KR, et al. The protein kinase C $\beta$ -selective inhibitor, Enzastaurin (LY317615.HCl), suppresses signaling through the AKT pathway, induces apoptosis, and suppresses growth of human colon cancer and glioblastoma xenografts. *Cancer Res* 2005;65: 7462–9.
10. Fine H, Kim L, Royce C, et al. Results from phase II trial of Enzastaurin (LY317615) in patients with recurrent high grade gliomas. *Proc Am Soc Clin Oncol* 2005;23:1504a.
11. Querfeld C, Rizvi MA, Kuzel TM, et al. The selective protein kinase C $\beta$  inhibitor enzastaurin induces apoptosis in cutaneous T-cell lymphoma cell lines through the AKT pathway. *J Invest Dermatol* 2006;126:1641–7.
12. Goldman-Leikin RE, Salwen HR, Herst CV, et al. Characterization of a novel myeloma cell line, MM.1. *J Lab Clin Med* 1989;113:335–45.
13. Lichtenstein A, Tu Y, Fady C, Vescio R, Berenson J. Interleukin-6 inhibits apoptosis of malignant plasma cells. *Cell Immunol* 1995;162: 248–55.
14. Akira S, Taga T, Kishimoto T. Interleukin-6 in biology and medicine. *Adv Immunol* 1993;54:1–78.
15. Hardin J, MacLeod S, Grigorieva I, et al. Interleukin-6 prevents dexamethasone-induced myeloma cell death. *Blood* 1994;84:3063–70.
16. Georgii-Hemming P, Wiklund HJ, Ljunggren O, Nilsson K. Insulin-like growth factor I is a growth and survival factor in human multiple myeloma cell lines. *Blood* 1996;88:2250–8.
17. Xu F, Gardner A, Tu Y, Michl P, Prager D, Lichtenstein A. Multiple myeloma cells are protected against dexamethasone-induced apoptosis by insulin-like growth factors. *Br J Haematol* 1997;97:429–40.
18. Drew L, Kumar R, Bandyopadhyay D, Gupta S. Inhibition of the protein kinase C pathway promotes anti-CD95-induced apoptosis in Jurkat T cells. *Int Immunol* 1998;10:877–89.
19. Gschwendt M. Protein kinase C $\delta$ . *Eur J Biochem* 1999;259:555–64.
20. Jarvis WD, Turner AJ, Povirk LF, Traylor RS, Grant S. Induction of apoptotic DNA fragmentation and cell death in HL-60 human promyelocytic leukemia cells by pharmacological inhibitors of protein kinase C. *Cancer Res* 1994;54:1707–14.
21. Tenzer A, Zingg D, Rocha S, et al. The phosphatidylinositol 3'-kinase/Akt survival pathway is a target for the anticancer and radiosensitizing agent PKC412, an inhibitor of protein kinase C. *Cancer Res* 2001;61:8203–10.
22. Mitsiades CS, Mitsiades N, Poulaki V, et al. Activation of NF- $\kappa$ B and upregulation of intracellular anti-apoptotic proteins via the IGF-I/Akt signaling in human multiple myeloma cells:therapeutic implications. *Oncogene* 2002;21:5673–83.

# Molecular Cancer Therapeutics

## Enzastaurin (LY317615), a protein kinase C $\beta$ inhibitor, inhibits the AKT pathway and induces apoptosis in multiple myeloma cell lines

Mujahid A. Rizvi, Kulsoom Ghias, Katharine M. Davies, et al.

*Mol Cancer Ther* 2006;5:1783-1789.

**Updated version** Access the most recent version of this article at:  
<http://mct.aacrjournals.org/content/5/7/1783>

**Cited articles** This article cites 22 articles, 6 of which you can access for free at:  
<http://mct.aacrjournals.org/content/5/7/1783.full#ref-list-1>

**Citing articles** This article has been cited by 14 HighWire-hosted articles. Access the articles at:  
<http://mct.aacrjournals.org/content/5/7/1783.full#related-urls>

**E-mail alerts** [Sign up to receive free email-alerts](#) related to this article or journal.

**Reprints and Subscriptions** To order reprints of this article or to subscribe to the journal, contact the AACR Publications Department at [pubs@aacr.org](mailto:pubs@aacr.org).

**Permissions** To request permission to re-use all or part of this article, use this link  
<http://mct.aacrjournals.org/content/5/7/1783>.  
Click on "Request Permissions" which will take you to the Copyright Clearance Center's (CCC) Rightslink site.